

Adsorption Performance of Packed Bed Column for the Removal of Lead (II) using Velvet Tamarind (*Dialium indum*) Shells

Jibrin Noah Akoji

Department of Petroleum Chemistry

Baze University, Abuja

Corresponding Author: noah.akoji@bazeuniversity.edu.ng

Abstract

The removal of Pb ions by activated carbons prepared from velvet tamarind (*Dialium indum*) shells was studied to investigate its uptake potentials using column sorption at different operating conditions (flow rates, initial concentrations and bed height). The prepared adsorbent was characterized by determining the physicochemical properties, proximate analysis, carbon, Hydrogen, Nitrogen and Sulphur analysis, Fourier Transform-Infra Red, Potentiometric titration. Different dynamic models were used to describe the sorption processes. The FTIR analysis results suggested the presence of functional groups such as hydroxyl, carbonyl, carboxyl and amine which could bind the metals and remove them from the solution. The values of moisture content, volatile matter, fixed carbon and ash content as obtained from % proximate analysis are 3.43, 27.07, 65.05, 4.45 for activated carbons prepared from velvet tamarind shells. Ultimate analysis revealed that activated carbons prepared from velvet tamarind shells contained 75% carbon. The surface area and Iodine number of activated carbon from velvet tamarind shell are $570 \text{ m}^2\text{g}^{-1}$ and 614.7 mgg^{-1} respectively. The column experimental data revealed that an increase in bed height and initial metal concentration or a decrease of flow rate enhances the longevity of column performance by increasing both breakthrough time and exhaustion time thereby delaying bed saturation. Low ash content and high surface areas are indication of good mechanical strength and microporosity of the activated carbons prepared from this precursor. The activated carbons are inexpensive and appeared to be effective and can be explore for future commercial application for environmental sustainability.

Key words: Adsorbent; velvet tamarind; adsorption; Pollution;

1. INTRODUCTION

The exponential increase in the world population as well as increase in industrial activities made environmental pollution an important issue of serious concern. Gaseous, liquid and solid wastes emanates from these activities. Earth's surface is made up of 70% water which is the most valuable natural resource existing on our planet without which life becomes impossible. Although this fact is widely recognized, pollution of water resources is a common problem being faced today. Lakes, rivers and oceans are being overwhelmed with many toxic contaminants [1].

Among toxic substances exceeding threshold levels are heavy metals and water pollution by heavy metals occurs directly by effluent discharge from industries such as textiles, dyes, leather tanning, electroplating, metal finishing, refineries, mine water and waste treatment plants and indirectly by the contaminants that enter the water supply from soils/ground water systems and from the atmosphere via rain water. The presence of these toxic substances in an undesirable level in wastewaters makes their removal to receive much attention [2]. When heavy metal concentration

38 in waste water is considerably high, it would endanger public health and the environment if discharged into the
39 environment without adequate treatment [3].

40 Several methods such as ion exchange, solvent extraction, reverse osmosis, and precipitation have been used for the
41 removal of heavy metals from aqueous solutions but most of these methods are non-economical and have many
42 disadvantages such as high reagents and energy requirements, generation of toxic sludge of other waste products that
43 also require disposal after treatment [4]. However, adsorption of heavy metals from aqueous solutions is a well
44 established process that has proven very efficient and promising in the removal of contaminants from aqueous
45 effluents where interactions between metal ions and biomass present potential applications for the remediation of
46 metal contaminated waters in various industries [3]. The process of adsorption has an edge over other methods due to
47 its sludge free clean operation and efficient removal of toxic metals even from dilute solution. It is as an innovative
48 principle of using waste to treat waste and will be more efficient because the agricultural by-products used as
49 adsorbents are readily available, affordable, eco-friendly and have high uptake capacity for heavy metals due to the
50 presence of functional groups which can bind metals to effect their removal from effluents making it more cost effective
51 than the use of commercial activated carbon which is expensive. Alternative activated carbon produced from velvet
52 tamarind fruits will be cheap, locally available and could be used to reduce environmental pollution by heavy metals.

53 The release of toxic metals into the environment would be controlled in this way, and so, the process could be used
54 more extensively as an alternative method to the conventional treatment techniques [5].

55 Considerable attention has been devoted to the development of unconventional materials like used agricultural by-
56 products for the removal of heavy metals from waste water [6], since these plant based by-products represent waste
57 resources, and are widely available and environmentally friendly [7]. Various natural adsorbents obtained from
58 agricultural wastes like sun flower stalk, Eucalyptus bark, maize husk, coconut shell, waste tea, rice straw, tree leaves,
59 peanut and walnut husk, palm fruit bunch and African spinach stalk have been tried as raw materials for adsorbents to
60 achieve effective removal of various heavy metals[8][9].

61 Commercial activated carbons have been used for the removal of heavy metals but are imported and expensive. There
62 is a need to look for viable non-conventional low-cost adsorbents as alternative to commercial activated carbon in
63 order to meet the growing demand for cheaper and effective adsorbents. Velvet tamarind is among common fruits
64 produced in Nigeria and large volumes of its non-edible and non useful parts such as the shells constitute
65 environmental problems. These non essential parts of velvet tamarind could be explored for the production of activated
66 carbon.

67 The aim of this study is to prepare, characterize and assess the heavy metal adsorption potentials of activated carbons
68 produced from velvet tamarind.

69 **2. Materials and Methods**

70 **2.1 Sample Collection and Preparation**

71 The carbonaceous precursor used for preparation of activated carbon is velvet tamarind shells that were obtained as
72 agricultural and forest wastes. Prior to use, samples were washed gently with water to remove mud and other impurities
73 present on the surface and then sundried for one week. The samples shells collected after discarding the fruit pulp, were
74 washed with deionized water, sun dried and then dried in a vacuum oven at 80°C for 24 h, crushed and ground using
75 mortar and pestle. The particles were separated by using a US standard testing sieve (No. 100~No. 200). 100 g of raw
76 material was impregnated with 100 cm³ of concentrated H₂SO₄ for 12 h. The impregnation was carried out at 70 °C in a
77 hot air oven to achieve well penetration of chemical into the interior of the precursor. The sieved samples were placed in
78 a crucible and heated in a muffle furnace for 60 min at 500°C. Activated carbons produced were cooled in desiccators and
79 rinsed with deionized water until neutral pH was attained and stocked for subsequent heavy metal removal tests and
80 analysis.

81 2.2 Sample Characterization

82 The pH, bulk density, iodine number, specific surface area, chemical composition of the adsorbents, proximate
83 analysis of the activated carbons were determined using standard test [10][11][12][13]. Ultimate analysis (CHNS
84 elemental analysis) of the samples were determined by subjecting them to combustion process (furnace at ca. 1000°C)
85 for 30 min, where carbon was converted to carbon dioxide; hydrogen to water; nitrogen to nitrogen gas/ oxides of
86 nitrogen and sulphur to sulphur dioxide. The combustion products were swept out of the combustion chamber by inert
87 carrier gas and passed over heated (about 600° C) high purity copper situated at the base of the combustion chamber
88 to remove any oxygen not consumed in the initial combustion and to convert any oxides of nitrogen to nitrogen gas.
89 The gases were then passed through the absorbent traps in order to leave carbon dioxide, water, nitrogen and sulphur
90 dioxide which were separated and detected using GC and thermal conductivity detection.

91

92 2.3 Fourier Transform Infrared (FTIR) Spectrometer

93 FTIR analysis was made using IPRestige-21, FTIR-84005, SHIMADZU Corporation (Kyoto, Japan). Sample of 0.1 g
94 was mixed with 1 g of KBr, spectroscopy grade (Merk, Darmstadt, Germany), in a mortar. Part of this mix was
95 introduced in a cell connected to a piston of a hydraulic pump giving a compression pressure of 15 kPa / cm². The mix
96 was converted to a solid disc which was placed in an oven at 105°C for 4 h to prevent any interference with any
97 existing water vapor or carbon dioxide molecules. Then it was transferred to the FTIR analyzer and a corresponding
98 spectrum was obtained showing the wave lengths of the different functional groups in the sample which were identified
99 by comparing these values with those in the library.

100 2.4 Preparation of Pb Solution (Simulated Effluent)

101 Standard lead (Pb) stock solution (1000 mgdm⁻³) was prepared by placing 1.578 g Pb(NO₃)₂ in a volumetric flask to
102 which 100 cm³ of deionized water was added. The flasks were shaken vigorously to ensure the dissolution of the
103 mixture. The solution was made up to 1000 cm³ mark with deionized water. The working concentrations were prepared

104 from the stock solution by serial dilution. pH adjustment of solutions was made using dilute NaOH and HCl solutions.
 105 Deionized water was used to prepare all the solutions. All reagents were of analytical grade.

106

107 2.5 Fixed Bed Column Experimental Procedure

108 Fixed bed column studies were carried out using a glass column of 30 mm internal diameter and 400 mm length. The
 109 activated carbon having 0.425 to 0.600 mm particle size range was used. The activated carbon was packed in the
 110 column with a layer of glass wool at the top and bottom. Bed height of 50, 100 and 150 mm were used. The tank
 111 containing the heavy metal solution was placed at a higher elevation so that the metal solution could be introduced into
 112 the column by gravitational flow. The flow controller helps to regulate the flow rate. Three flow rates (1, 3 and 5
 113 cm³min⁻¹) were used while initial ion concentrations of 50, 100 and 150 mgdm⁻³ were used. The effluent samples were
 114 collected at hourly intervals and analyzed for the residual metal concentration using atomic absorption
 115 spectrophotometer.

116 2.6 Dynamic models of Column Adsorption of lead (Pb) onto activated carbon from Velvet 117 Tamarind (*Dialium indum*) Shells

118 For the successful design of a column adsorption process, it is important to predict the concentration-time profile or
 119 breakthrough curve for effluent parameters. A number of mathematical models have been developed for use in the
 120 design of continuous fixed bed sorption columns. In this work, the Bed Depth Service Time (BDST), Thomas and
 121 Yoon-Nelson models were used in predicting the behavior of the breakthrough curve because of their effectiveness.
 122 The model's equations are presented in Equations 1 to 3:

$$123 \text{BDST} = t = \frac{N_0}{C_0 F} Z - \frac{1}{K a C_0} \ln \left(\frac{C_0}{C_B} \right) - 1 \quad (1)$$

$$124 \text{Thomas} = \ln \left(\frac{C_0}{C_t} - 1 \right) = \frac{K t h q_0 M}{Q} - K t h C_0 t \quad (2)$$

$$125 \text{Yoon-Nelson} = \ln \left(\frac{C_t}{C_0 - C_t} \right) = K_y n t - \tau K_y n \quad (3)$$

126

127 The maximum column capacity, q_{total} (mg) for a bed height of 10.00 cm, initial metal concentration of 50.00 mg/dm³ and
 128 flow rates of 1, 3 and 5 cm³min⁻¹ was calculated from the area under the breakthrough curves as given by the Equation
 129 4 (Ahmad and Hameed, 2010)

130

$$131 q_{\text{total}} = \frac{QA}{1000} = \frac{Q}{1000} \int_{t=0}^{t=\text{total}} C_{ad} dt \quad (4)$$

132

133 where $C_{ad} = C_i - C_e$ (mg L⁻¹), $t = \text{total}$ is the total flow time (min), Q is the flow rate (cm min⁻¹) and A is the area under
 134 the breakthrough curve (cm²).

135

136 The equilibrium uptake ($q_{e(\text{exp})}$), i.e. the amount of the metals adsorbed (mg) per unit dry weight of adsorbent (mgg⁻¹) in
 137 the column, was calculated from Equation 5 (Martin-Lara *et al.*, 2012):

$$138 q_{e(\text{exp})} = \frac{qt_{\text{total}}}{W} \quad (5)$$

139 where W is the total dry weight of velvet tamarind shell in the column (g)
140 The total volume treated, V_{eff} (cm^3) was calculated from Equation 6 (Futalan *et al.*, 2011)

$$141 \quad V_{\text{eff}} = Q_{t_{\text{total}}} \quad (6)$$

142 The mass transfer zone (Z_m) is one of the widely used parameters to examine the effects of the column adsorption
143 height. To determine the length of the adsorbent zone in the column, Z_m was calculated from Equation 7:

$$144 \quad Z_m(\text{cm}) = Z(t_e - t_b/t_e) \quad (7)$$

145 where, L presents the closed height (cm), t_b is the time (minute) required to reach the breakthrough point or $C_{\text{eff}}/C_0 =$
146 0.05 and t_e is the time (minute) required to reach the exhaustion point or $C_{\text{eff}}/C_0 = 0.95$ (Apiratikul and Pavasant,
147 2008).

148 3.0 RESULTS AND DISCUSSION

149 The proximate analysis, ultimate analysis and physicochemical properties of activated carbons produced from velvet
150 tamarind shells are presented in Tables 1, 2 and 3

151 **Table 1. Proximate analysis, of the activated carbons prepared from velvet tamarind shells**

Property	Vt
Moisture	3.43
Volatile Matter	27.07
Fixed carbon	65.05
Ash	4.45

153 Vt = activated carbon from velvet tamarind fruit shells

155 **Table 2. Ultimate Analysis of Activated Carbons from Velvet Tamarind Fruit Shells**

Element	Vt
C	75
H	1.2
N	1.8
S	0.8
O	21.5

156

157

158

159

160 **Table 3. Physicochemical Properties of Activated carbons prepared from Velvet Tamarind shells.**

Parameter	Vt
Bulk density (gcm ³)	0.51
Iodine number (mgg ⁻¹)	614.7
Surface area (m ² g ⁻¹)	570
Particle density (gcm ³)	0.72
Porosity (%)	26.4
pH	6.9
Pore Volume	0.13

161

162 **3.1 Proximate and ultimate analysis of activated carbons from velvet tamarind shells**

163 According to [14], ash content is the measurement of the amount of mineral (e.g. Ca, Mg, Si and Fe) in activated
 164 carbon. Ash content obtained in this work was 4.45 for activated carbons prepared from velvet tamarind shells (Table
 165 1). The ash content of this carbon is well below the typical ash content values of 8-12% obtained by [15] and 12%
 166 obtained by [16] but higher than the 3.58 and 4.89 obtained by [17] and [18] for coconut and Bael fruit shell
 167 respectively. Typical ash content of activated carbons is around 5-6 % [19]. A small increase in ash content causes a
 168 decrease in adsorptive properties of activated carbons by reducing the mechanical strength of carbon and affects
 169 adsorptive capacity. The presence of ash has been shown to inhibit surface development [20].

170

171 The value of 78 and 65.05% fixed carbon were obtained from percentage ultimate and proximate analysis of activated
 172 carbon prepared from velvet tamarind fruit shells (Table 1&2). [21] prepared activated carbon from *Euphorbia*
 173 *antiquorum* and obtained 57.94% fixed carbon. [22] reported values ranging from 23.7 to 87.13% within 450 to 950°C.
 174 Carbonization leads to carbon atoms rearrangement into graphitic-like structures and the pyrolytic decomposition of the
 175 precursor and non-carbon species elimination, resulting in a fixed carbonaceous char produced [23]. Also activating
 176 agents act as dehydrating agents and oxidants which also influence the pyrolytic decomposition and prevent the
 177 formation of the tar or ash, hence developing the carbon yield. The combine influence of activation and carbonization
 178 increases carbon yield.

179

180 As reported in Table 3, the following; 0.51 g/cm³, 614.7 mg/g, 570 m²/g, 26.4% were obtained as the values of bulk
 181 density, iodine number, surface area and porosity for activated carbon prepared from Velvet Tamarind shells. The
 182 values of bulk density, surface area, and iodine number were similar to the values obtained by [24][26] produced

183 activated carbon from palm kernel shell and obtained yields of bulk density of $0.5048\text{g}/\text{cm}^3$, iodine number of 766.99
184 mgg^{-1} and $669.75\text{ m}^2\text{g}^{-1}$ BET surface area. Bulk density is the weight per unit volume of dry carbon in a packed bed
185 and is 80-85% of the apparent density [27]. Higher density provides greater volume activity and normally indicates
186 better quality activated carbon. [28] in his comparative adsorption studies for the removal of copper (II) from aqueous
187 solution by different adsorbent obtained bulk density values ranging from 0.32 to 0.62 gcm^{-3} . Bulk density of 0.48 gcm^{-3}
188 3 was obtained by [21] and is lower than 0.51 gcm^{-2} obtained for velvet tamarind shells.

189

190 The iodine number value is an indication of surface area of the activated carbon [29]. Activated carbons with iodine
191 numbers of about 550 mgg^{-1} can be attractive for waste water treatment from the user's viewpoint [30]. The iodine
192 number values of 614.7 mgg^{-1} were obtained for activated carbon prepared from velvet tamarind fruits shells (Table 3).
193 These results were within the range of 608 and 746 mgg^{-1} obtained by [31]. Analysing the iodine number of activated
194 carbon prepared from palm-oil shell by pyrolysis and steam activation in a fixed bed reactor, [25] obtained maximum
195 value of 766.99 mgg^{-1} at 750°C . According to [13], each 1.0mg of iodine adsorbed is ideally considered to represent
196 1.0 m^2 of activated carbon internal area. Therefore, the adsorbents have enough internal surface area for adsorption.

197 **3.2 Surface area of activated carbons from velvet tamarind fruit shells**

198 Surface area is the carbon particle area available for adsorption. In general, the larger the effective surface area, the
199 greater is the adsorption capacity. A surface area of the activated carbons used in this study is as reported in Table 4.
200 . The results indicated that the surface area of $570\text{ m}^2\text{g}^{-1}$ was obtained for velvet tamarind shells activated carbon. The
201 specific surface area as indicated in Table 4. further confirmed the porous nature of the activated carbons. According
202 to [32], an adsorbent with a surface area of $500\text{ m}^2\text{g}^{-1}$ and above has a well formed microporous structures suitable for
203 adsorption. According to [31], 95% of the total surface areas of a given adsorbent are micropores. [33] stated that most
204 widely used commercial activated carbon has surface areas of between 600 - $1000\text{ m}^2\text{g}^{-1}$.

205 **3.3 pH of activated carbons from velvet tamarind fruit shells**

206 The pH of activated carbon can be defined as the pH of a suspension of carbon in distilled water. The chemical nature
207 of the carbon surfaces is mostly deduced from the acidity or pH of the carbon. Table 4 presented the pH of the
208 activated carbon prepared from velvet tamarind fruits shells as 6.9 . The results suggest weakly acidic surface
209 properties. Similar results were obtained by [34]. [20] obtained pH between 6.4 and 7.4 for activated carbon prepared
210 from bagasse.

211 **3.4 Moisture content of activated carbons from velvet tamarind shells**

212 Moisture content was measured from loss of water over initial weight of raw materials. Usually moisture content
213 decreases as the temperature increases. As presented in Table 4, moisture content of 3.43% was obtained for the

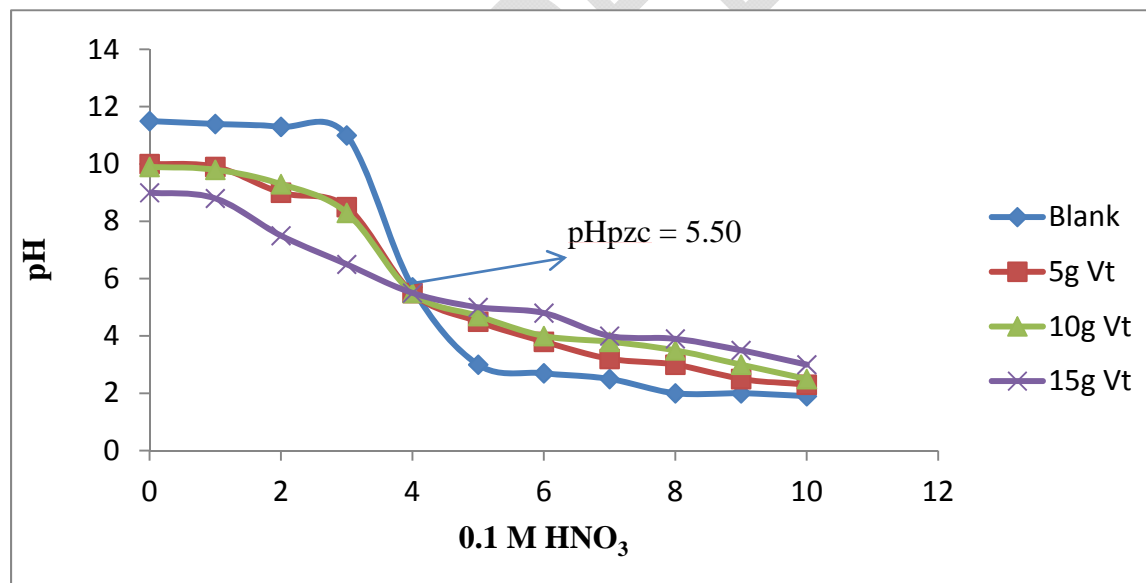
214 activated carbon prepared from Velvet tamarind fruits shells. [25] obtained values between 8.35 to 11.38% for moisture
215 content while [16] obtained 4.33% in their work. The moisture contents of commercial activated carbons ranged
216 between 2- 10 % [33]. The practical limit for the level of moisture content allowed in the activated carbon varies within 3
217 to 6% [6]. The moisture content of 3.43% obtained for the activated carbon prepared from Velvet tamarind fruits shells
218 activated carbons therefore fall within the practical limit.

219 3.5 Volatile matter of activated carbons from velvet tamarind shells

220 The values of volatile matter of 27.07% (Table 1.) was obtained for Velvet tamarind fruit shells activated carbons. Lou
221 *et al.* (1999) studied chars prepared from oil palm waste and obtained % volatile matter ranging from 74.86 to 4.08%
222 between 450 to 950°C.

223 3.6 Potentiometric titration curves of activated carbons from velvet tamarind fruit shells

224 Figures 1. indicate the result of potentiometric curves of the activated carbons investigated to determine the Point of
225 Zero Charge on the surface of the adsorbent. The point of zero charge (PZC) is an adsorption phenomenon which
226 describes the condition when the electrical charge density on a surface is zero. The common intersection point of the
227 titration curves with the blank is the pH at PZC (pH_{PZC}). From the curves (Figure 1), the pH_{PZC} for activated carbon
228 prepared from velvet tamarind shells was identified as 5.50.
229



231

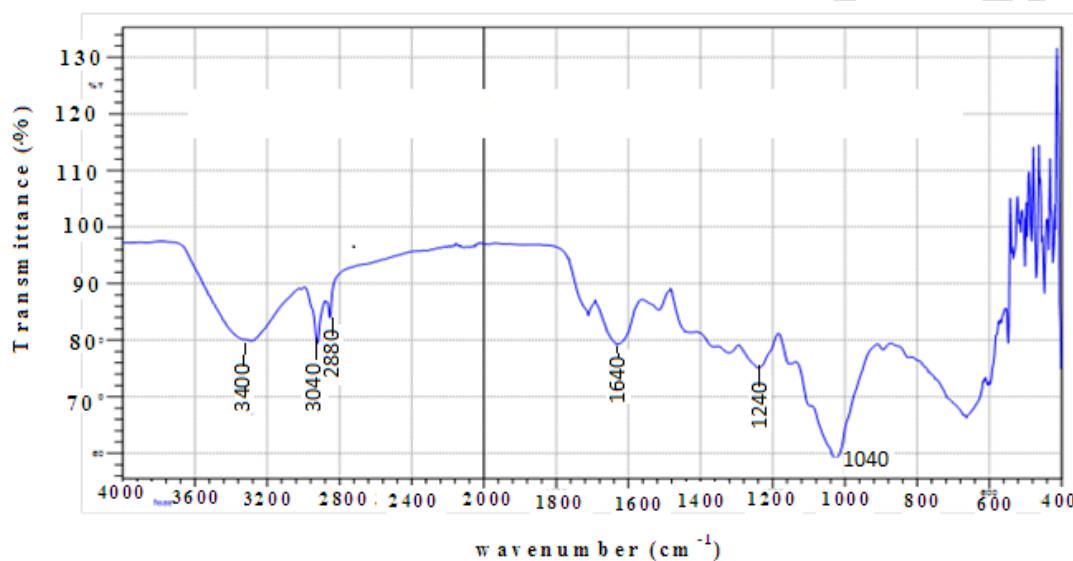
232 **Figure 1: Potentiometric Titration Curves of Activated Carbon from Velvet Tamarind Shell**

233

234 The titration curve of Velvet tamarind shells is a bit steep. This indicates a moderate capacity of the shells to take up
235 protons (buffering capacity). Therefore, the capacity to take up cationic metals by ionic exchange is probably also
236 moderate. Any pH above pH(pzc) provide a negatively charged surface favourable for adsorption of cationic heavy
237 metals from the solution.

238 3.7 Fourier transforms infrared spectrometer (FTIR) result of activated carbons from velvet 239 tamarind

240 The FTIR spectral of activated carbons prepared from velvet tamarind fruit shells were used to determine the vibration
241 frequency changes in the functional groups on the surface which facilitates the adsorption of metal ions. The spectra of
242 the activated carbons were measured within the range of 400 – 4000 cm^{-1} wave number as shown in Figures 2.
243



244

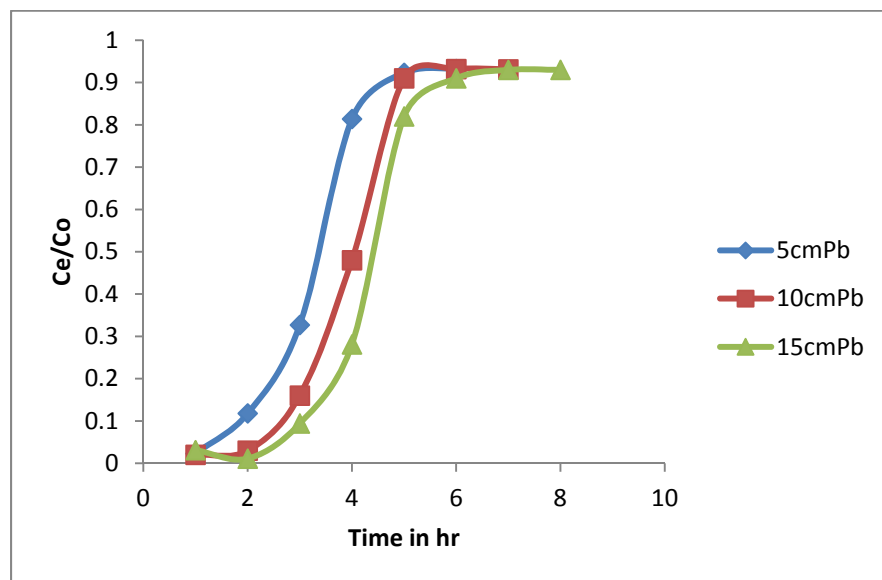
245 **Figure 2: FTIR Spectrum of Activated carbon prepared from Velvet Tamarind Shell**

246 The FTIR analysis result (Figure 2.) suggest the presence of such functional groups as the carboxylic acid or alcoholic
247 O-H bond stretching which may overlap with amine (N-H) bond stretching at peaks between 3250-3400 cm^{-1} ; possible
248 C=O bond of carbonyl or amide groups within 1640-1670 cm^{-1} ; C-O and O-H bond stretching of alcohol and ethers at
249 1000-1260 cm^{-1} of the finger-print region (Gimba et al, 2001). The important parameters that influence and determine
250 the adsorption of metal ions from aqueous solutions are the carbon-oxygen functional groups present on the carbon
251 surface and the pH of the solution (Bansal and Goyal, 2005).
252

253 3.8 Column Adsorption Studies of Lead (Pb) on Activated carbon Prepared from Velvet Tamarind 254 Shells

255 3.8.1 Effect of bed height

256 The adsorption of metal ions in the packed bed column is largely dependent on the bed height, which is directly
257 proportional to the quantity of adsorbent in the column. The effect of bed height on breakthrough curve analysis was
258 studied by varying the bed height from 5 cm to 15 cm at increment of 5 cm. The adsorption breakthrough curves were
259 obtained by varying the bed heights at a flow rate of $1\text{cm}^3/\text{min}$ and an inlet Pb ions concentration of $50\text{mg}/\text{dm}^3$. The
260 breakthrough curves are presented in Figures 2. Faster breakthrough curves were observed for a bed height of 5 cm
261 compared to the bed height of 10 cm and 15 cm.



262
263 **Figure 3: Column adsorption of Pb(II) by Activated Carbon from Velvet Tamarind Fruits Shells at different Bed**
264 **height**

265
266 As depicted by Figure 3, the breakthrough time varied with bed height. Steeper breakthrough curves were achieved
267 with a decrease in bed depth. The breakthrough time decreased with a decreasing bed depth from 15 to 5 cm, as
268 binding sites were restricted at low bed depths. At low bed depth, the metal ions do not have enough time to diffuse
269 into the surface of the adsorbents, and a reduction in breakthrough time occurs. Conversely, with an increase in bed
270 depth, the residence time of metal ions solution inside the column was increased, allowing the metal ions to diffuse
271 deeper into the adsorbents.

272
273 The results indicate that the throughput volume of the aqueous solution increased with increase in bed height, due to
274 the availability of more number of sorption sites [21]. At higher bed depth of 10 cm, adsorbent mass was more residing
275 in the column thereby providing larger service area for binding, fixation, diffusion and permeation of the solute to the
276 adsorbent. Longer bed depth also provided more reaction area and larger volume of influent treatment which translated
277 to higher adsorption capacity.

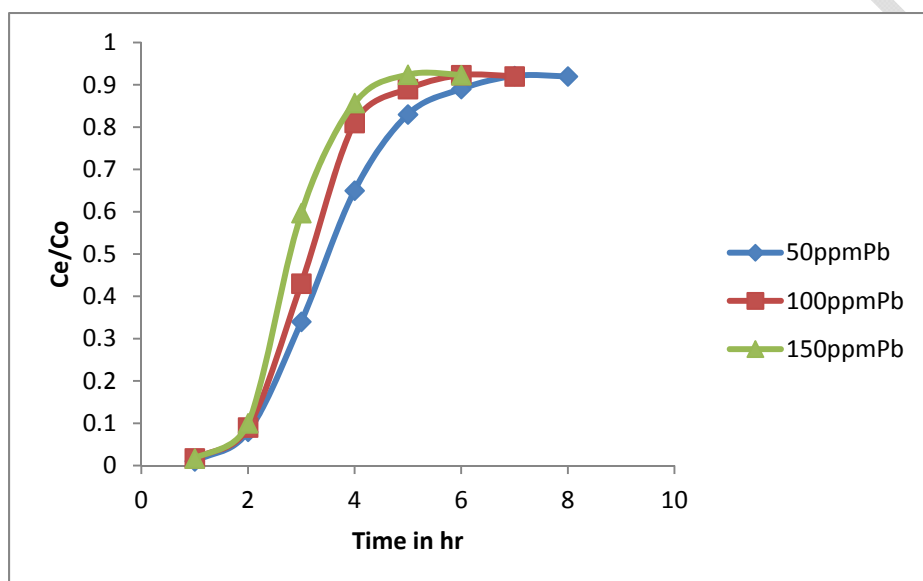
278

279 The equilibrium sorption capacity decreased with increase in bed height. This shows that at smaller bed height, the
280 effluent adsorbate concentration ratio increased more rapidly than for a higher bed height. Furthermore, the bed is
281 saturated in less time for smaller bed heights. The slope of the S-shape from t_b to t_e decreased as the bed height
282 increased from 5 to 15 cm, indicating the breakthrough curve becomes steeper as the bed height decreased. Also the
283 breakthrough time (t_b) and exhaustion time (t_e) increase with increase in bed depth

284 3.8.2 Effect of Initial Metal Concentration

285 A Series of column experiments with different metals concentrations namely, 50, 100 and 150 ppm were conducted to
286 investigate the effect of initial metal concentration on the performance of the fixed-bed operation. Figure 3 presented
287 the breakthrough curves for the adsorption of Pb onto Velvet tamarind fruit shells activated carbon at various initial
288 metal concentrations.

289 .



290

291 **Figure 4: Column adsorption of Pb(II) by Activated Carbon from Velvet Tamarind Fruit shells at different**
292 **Initial Concentration.**

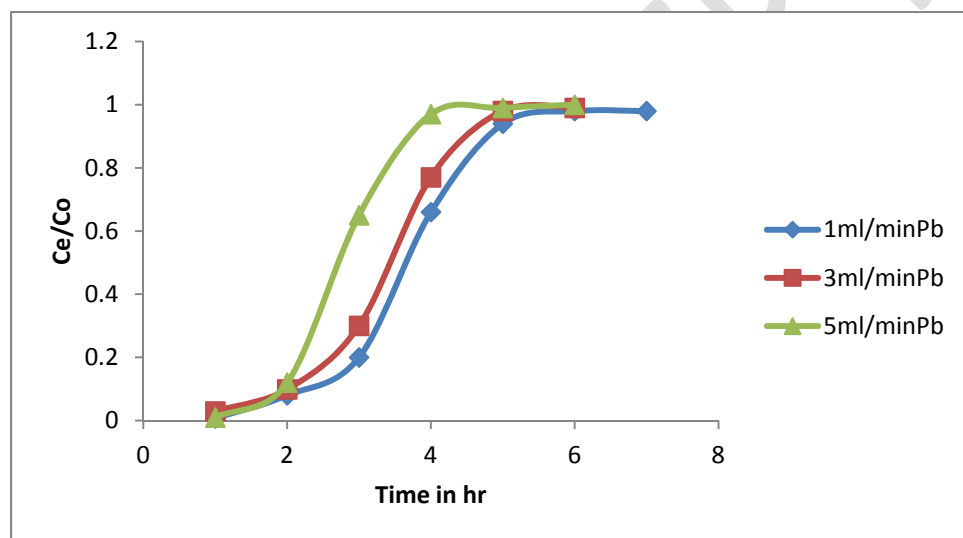
293 .

294 It can be seen from the Figure 4 that breakthrough curves display three important features: an initial lag period during
295 which effluent metal ions are non-detectable, followed by a rise in concentration, and finally a period of slow increase in
296 effluent level. It was assumed that the breakthrough metal-concentration would be 5% of the influent concentration. It is
297 evident that by increasing initial metal concentration, the slope of the breakthrough curve increased and became much
298 steeper, hence reducing the volume which can be treated before breakthrough occurred. This is due to the fact that by
299 increasing the initial metal concentration, the driving forces increases which enhance the rate of metal adsorption and
300 saturates the binding sites more quickly. This is consistent with results of the finding of [35], where the authors found
301 that by increasing inlet adsorbate concentration, the slope of the breakthrough curve increased and the volume treated

302 before carbon regeneration reduced. This behaviour was attributed to the high concentrations which saturated the
303 activated carbon more quickly, thereby decreasing the breakthrough time. It is also clear from Figures 1. to 5. that all
304 the curves exhibit a characteristic “S” shape which indicates an effective use of adsorbent [36].

305 3.8.3 Effect of flow rate on breakthrough curves

306 The adsorption columns were operated with different flow rates (1, 3 and 5 cm³/min) until no further metal ions removal
307 was observed. The adsorbent bed height and inlet initial metal ions concentration were fixed at 10 cm and 50 mg/dm³,
308 respectively. The breakthrough curve for a column was determined by plotting the ratio of the C_e/C_0 (C_e and C_0 are
309 the metal ions concentration of effluent and influent, respectively) against time, as shown in Figures 5. The effect of
310 the flow rate on the adsorption of Cu, Cd, Pb and Ni are shown as breakthrough curves in the figures. It was observed
311 that breakthrough generally occurred faster with higher flow rate. The reason is that at higher flow rate, the rate of
312 mass transfer increased, thus the amount of metal ions adsorbed onto the unit bed height (mass transfer zone)
313 increased [37]. In addition, the adsorption capacity decreases with increase in flow rates due to insufficient residence
314 time of the solute in the column and lack of diffusion of the solute into the pores of the adsorbent, therefore the solute
315 left the column before equilibrium occurred. These results were in agreement with other findings as reported by [38].
316



317

318 **Figure 5: Column adsorption of Pb(II) by Activated Carbon from Velvet Tamarind Fruits Shell Activated**
319 **Carbon at different Flow rate.**

320

321 The column performed well at the lowest flow rate (1cm³/min). Earlier breakthrough and exhaustion times were
322 achieved, when the flow rate was increased from 1 to 5 cm³/min. This was due to a decrease in the residence time,
323 which restricted the contact of metal ions to the adsorbents. Similar results have been found for As (III) removal in a

324 fixed-bed system using modified calcined bauxite and for color removal in a fixed-bed column system using surfactant-
325 modified zeolite [39].

326 **3.9 Column Kinetic Study**

327 Three models (Thomas model and Yoon-Nelson) were used to analyze the column performance.

328 **3.9.1 Thomas model**

330 The model was applied to the experimental data with respect to the initial metals concentration, flow rate and bed
331 height. The kinetic coefficient, k_{Th} and the adsorption capacity of the bed, q_0 were determined from the plot of
332 $\ln\left(\frac{C_0}{C_e} - 1\right)$ against t . The results of k_{Th} , R^2 and q_0 are given in Table 4.. The results showed that the kinetic coefficient
333 k_{Th} is dependent on flow rate, initial ion concentration and bed height. The maximum adsorption capacity q_0 and
334 Kinetic coefficient k_{Th} decreased with increase in flow rate but increased with increase in bed height and initial ion
335 concentration. The values of k_{Th} obtained in this work is similar to the ones obtained by [15]. High values of regression
336 coefficients were obtained indicating that the kinetic data conformed well to Thomas model in contrast with the report of
337 [40] but in agreement with the results obtained by [41]. The trend observed with the calculated values of k_{Th} , q_0 are in
338 agreement.

339 **3.9.2 Yoon and Nelson Model**

340 This model is based on the assumption that the rate of decrease in the probability of adsorption for each adsorbate
341 molecule is proportional to the probability of adsorbate adsorption and the probability of adsorbate breakthrough on the
342 adsorbent [42]. The Yoon and Nelson equation for single component system is expressed as shown in equation 4.3
343 [43]:

$$344 \ln \frac{C_e}{C_0 - C_e} = K_{yn}t - \tau K \quad (4.3)$$

345 Yoon and Nelson model has been used in the study of column adsorption kinetics [42][21]. The values of the Yoon-
346 Nelson parameters (K_{yn} and τ) were determined from the plot of $\ln \frac{C_e}{C_0 - C_e}$ versus t at various operating conditions (Table
347 4). A plot of $\ln \frac{C_e}{C_0 - C_e}$ versus t gives a straight line with slope of K_{yn} , and intercept of $-\tau K$. The results showed that the
348 rate constant, K_{yn} increased with increased inlet ions concentration, flow rate and bed height. The time required for
349 50% breakthrough, τ decreased with increase in flow rate and initial ion concentration. High values of correlation
350 coefficients obtained indicate that Yoon and Nelson model fitted well to the experimental data and can be used to

351 describe the Cd(II), Cu(II), Pb(II) and Ni(II)-Velvet Tamarind shell and Cd(II), Cu(II), Pb(II) and Ni(II) – Sandal fruit shell
352 biosorption system.

353

354

355

UNDER PEER REVIEW

356 Table 4 : Column kinetic parameters for Pb ions adsorption on activated carbon from Velvet tamarind fruit Shells

	Initial ion concentration(mg/dm ³)			Flow rates in cm ³ /min			Bed height (cm)		
	50	100	150	1	3	5	5	10	15
Thomas									
K _{Th} (cm ³ /min/mg)									
X10 ⁻³	2.40	7.20	2.30	0.34	0.38	0.64	0.24	0.42	0.42
q _o (mg/g)	1.20	1.93	2.80	0.71	0.38	2.10	1.00	1.20	1.80
R ²	0.98	0.97	0.95	0.98	0.99	0.98	0.96	0.95	0.99
Yoon & Nelson									
K _{yn} (min ⁻¹)									
X10 ⁻²	1.00	1.40	2.00	1.60	2.00	2.50	1.90	1.90	3.10
τ (min)	251.00	205.00	125.00	173.00	167.00	126.00	125.00	150.00	194.00
R ²	0.95	0.99	0.94	0.97	0.99	0.94	0.97	0.99	0.97

358 3.9.3 Lead Uptake in the Column at Different Operating Parameters

359 This study showed that the sorption uptake capacity of the column Pb 1.73 mg g⁻¹ for velvet tamarind fruit
360 shells activated carbon as shown in Table 5. The increased capacity of the column method is largely due to the
361 continuous increased concentration gradient in the interface of the adsorption zone as it passes through the
362 column, whereas the gradient concentration decreases with time in batch systems [44][45]

363

364 A characterisation study on the Velvet Tamarind shells prior to biosorption showed that hydroxyl and carboxylic
365 functional groups were present and might be involved in the removal of metal ions from aqueous solutions by
366 this biosorbent, besides micro precipitation and electrostatic attraction forces. The results obtained by [44] for
367 Ni(II), Cd(II), Zn(II) and Pb(II) ions using H₂SO₄ treated coconut shell suggest that a lower pH of 6 is required for
368 optimal removal of the studied metals, similar to the pH of 6 ± 0.2 used in this study.

369

370 **Table 5.: Uptake of Pb(II) by activated carbon from Velvet Tamarind Fruit shells at different flow rates**

	Z	Q	C ₀	V _{eff}	q _{total}	q _{e(exp)}	Z _m
	(cm)	(cm ³ min ⁻¹)	(mg dm ⁻³)	(cm ³)	(mg)	(mgg ⁻¹)	(cm)
V _t	10.00	1.00	50.00	1191.00	1.79	1.73	6.40
	10.00	3.00	50.00	882.00	0.44	1.64	7.95
	10.00	5.00	50.00	300.00	0.30	0.54	5.50

371

372

373 4.0 Conclusion

374 i. The experimental data revealed that an increase in bed height and initial metal concentration or a
375 decrease of flow rate enhances the longevity of column performance by increasing both breakthrough
376 time and exhaustion time thereby delaying bed saturation.

377 ii. The design of a continuous fixed bed column for removal of metal ions by velvet tamarind and sandal
378 fruit shells activated carbons can be achieved using the BDST, Yoon-Nelson and Thomas models.

379 iii. The FTIR analysis results suggested the presence of functional groups such as hydroxyl, carbonyl,
380 carboxyl and amine which could bind the metals and remove them from the solution.

381 iv. The values of moisture content, volatile matter, fixed carbon and ash content as obtained from %
382 proximate analysis are 3.43, 27.07, 65.05, 4.45 for activated carbons prepared from velvet tamarind
383 shells.

384 v. Ultimate analysis revealed that activated carbons prepared from velvet tamarind shells contained
385 75% carbon.
386

UNDER PEER REVIEW

387 **REFERENCES**

- 388 Oliveira, R. C., Guibal, E. & Garcia, O. Biosorption and desorption of lanthanum (III) and neodymium(III) in fixed-
389 bed columns with Sargassum sp. Perspectives for separation of rare earth metals. *Biotechnology Progress*,
390 2012;28(3), 715-722.
- 391 Ahluwalia, S. S., & Goyal, D. Removal of heavy metals by waste tea leaves from aqueous solution. *Engineering*
392 *and Life Science*, 2005;5(9),158-162.
- 393 Nouri, J., Mahvi, A. H., Babaei, A. A., Jahed, G. R., & Ahmadpour, E. Investigation of heavy metals in
394 groundwater *Pakistan Journal of Biological Science*, 2006;9(3), 377-384
- 395 Dermibas, A. Heavy metal adsorption onto agro-based waste materials: A review. *Journal of Hazardous*
396 *Material*, 2008;157(8), 220-229
- 397 Lazaridis, N. K., Matis, K. A., & Diels, L. (2005). 'Application of flotation to the solid/liquid separation of *Ralstonia*
398 *metallidurans*', 3rd *Eur. Bioremediation Conf.*, TU Crete, Chania,4-7 July.
- 399 Kuma, A., & Jena, H.M. High surface area microporous activated carbons prepared from Fox nut (*Euryale ferox*)
400 shell by zinc chloride activation *Applied Surface Science* 2015;356: 753-761.
- 401
- 402 Abia, A. A., & Asuquo, E. D. Kinetics of Cd²⁺ and Cr³⁺ Sorption from aqueous solution using mercaptoacetic
403 acid modified and unmodified oil palm fruit fibre (*elaeis guineensis*) adsorbents. *Journal of Tsinghua Science*
404 *Technology*, 2007;38(11),1324-1328.
- 405
- 406 Sing, K. S. W., Everett, D. H., Haul, R. A. W., Moscou, L., Pierotti, R. A., Rouquerol, J., & Siemieniowska, T.
407 Reporting Physisorption data for gas/solid interface with special reference to the determination of surface area
408 and porosity. *Pure and Applied Chemistry*. 2006;57, 603-619.
- 409 Kahraman, S., Dogan, N., & Erdemoglu, S. Use of various agricultural wastes for the removal of heavy metal
410 ions. *International Journal of Environmental Pollution*, 2008;34, 275-284.
- 411 American Society for Testing and Materials. Standard, Refractories, Carbon and Graphic Products; activated
412 Carbon, ASTM, Philadelphia, PA, 1996;15(01)
- 413 Ahmedna, M., Johns, M. M., Clarke, S. J., Marshall, W. E., & Rao, R. M. Potential of agricultural by-product-
414 based activated carbons for use in raw sugar decolourisation. *Journal of the Science of Food and Agriculture*,
415 1997;7(5),117-124.
- 416 American Society for Testing and Materials. Standard test method for determination of iodine number of
417 activated carbon. Philadelphia, PA: ASTM Committee on Standards.1986.
- 418 Al-Quodah, Z., & Shawabkah, R. Production and characterization of granular activated carbon from activated
419 sludge. *Brazilian Journal of Chemical Engineering*, 2009;26(1), 6-10.
- 420 Alam, C., Molina-Sabio, M., & Rodriguez-Reinoso, F. Adsorption of methane into ZnCl₂-activated carbon derived
421 discs. *Microporous and Mesoporous Materials*, 2008;76(15), 185-191
- 422 Yahaya, N. K. E. M., Abustana, I., Latiff, M. F. I. P. M., Bello, O. S. & Ahmad, M. A. Fixed-bed column study for
423 Cu (II) removal from aqueous solutions using rice husk based activated carbon. *International Journal of*
424 *Engineering & Technology*, 2011;11(1),248-252.
- 425 Maheswari, B. L., Mizon, K. J., Palmer, J. M., Korsch, M. J., Taylor, A.J., & Mahaffey, K.R. Blood lead changes
426 during pregnancy and postpartum with calcium supplementation. *Environmental Health Perspectives*,
427 2008;112(15),1499-1507.

- 428 Mozammel, H. M., Masahiro, O., & Bhattacharya, S. C. Activated charcoal from coconut shell using $ZnCl_2$
429 activation. *Biomass and Bioenergy*, 2010;22(6),397-400.
- 430 Gottipati, R., & Susmita, M. Process optimization of adsorption of Cr(VI) on activated carbons prepared from
431 plant precursors by a two-level full factorial design. *Chemical Engineering Journal*, 2012;160(1),99-107.
- 432 Pandey, K. K., Prasad, G., & Singh, V. N. Use of wollastonite for the treatment of Cu(II) rich effluent. *Water Air
433 and Soil Pollution*, 2014;27,287-296.
- 434 Valix, M., Cheung, W. H., & McKay, G. Preparation of activated carbon using low temperature carbonization
435 and physical activation of high ash raw bagasse for acid dye adsorption. *Chemosphere*, 2004;56, 493-501
- 436 Satyawali, Y., & Balakrishnan, M. Wastewater treatment in molasses-based alcohol distilleries for COD and
437 color removal: A review. *Journal of Environmental Management*, 2009;86, 481-497.
438
- 439 Lopez, F. A., Perez, C., Sainz, E., & Alonso, M. Adsorption of Pb (II) on blast furnace sludge, *Journal of
440 Chemical Technology*, 1995;62(2),200-206.
- 441 Kanan, K., & Sundaram, M. M. (2001). "Kinetics and mechanism of removal of methylene blue by adsorption on
442 various carbons—a comparative study", *Dyes and Pigments*. 51, 25–40.
- 443 Karthikeyan, S., Balasubramanian, R., & Iyer, C. S. P. Evaluation of the marine algae *Ulva fasciata* and
444 *Sargassum* species for the biosorption of Cu(II) from aqueous solutions. *Bioresource Technology*, 2008;98 (2),
445 452-455.
- 446 Vijayaraghavan, K., Padmesh, T. V. N., Palanivelu, K., & Velan, M. Biosorption of nickel(II) ions onto *Sargassum
447 wightii*: Application of two-parameter and three-parameter isotherm models. *Journal of Hazardous Materials*,
448 2006;133,304-308.
449
- 450 Mohammed, U. M., Binta, M., Mustapha, S., & Idris, M. Removal of Lead and Cobalt from Pharmaceutical
451 Effluent: Efficiency of Activated Coconut Shell and Commercial Activated Carbon. *American Chemical Science
452 Journal*, 2016;12(2),1-8
- 453 Alikarami, M., Abbari, Z., & Mohammadnezhad, S. Kinetics and thermodynamic studies of copper (II), mercury(II)
454 and chromium(II) adsorption from aqueous solution by peels of banana. *Journal of Basic and Applied Scientific
455 Research*, 2016;3(3), 8-15.
- 456 Amuda, O. S., Giwa, A. A., & Bello, I. A. Removal of heavy metal from industrial wastewater using modified
457 activated coconut shell carbon. *Biochemical Engineering Journal*, 2007;36(23), 174-181.
458
- 459 Deheyn, D. D., Gendreu, P., Baldwin, R. J., & Latz, M. I. Evidence for enhanced bioavailability of trace elements
460 in the marine ecosystem of Deception Island, a volcano in Antarctica. *Marine Environmental Research*,
461 2005;60(4),1-33.
462
- 463 Castro, A., Suarez-Garcia, F., Martinez-Alonso, A., & Tascon, J. M. D. (2008). Activated carbon fibers with a high
464 content of surface functional groups by phosphoric acid activation of PPTA. *Journal of Colloid and Interface
465 Science*, 2008;3(61),307-315.
- 466 Liu, S., & Liu, J. Surface modification of coconut shell based activated carbon for the improvement of
467 hydrophobic VOC removal. *Journal of Hazardous Materials*, 2008;192(2),683-690.
- 468 Yang, X., & Duri, B. A. (2005). "Kinetic modeling of liquid-phase adsorption of reactive dyes on activated carbon".
469 *Journal of Colloid Interface Sciences*, 2005;287,25-34.
- 470 Allothman, Z.A., Habila, M.A & Ali, R. (2011). Preparation of activated carbon using the copyrolysis of agricultural
471 and municipal solid wastes at a low carbonization temperature. In: Proceedings of the international conference
472 on biological and environmental chemistry: 2011;24,67–72

- 473 Betzy, N. T., & Soney., C. Cyanide in industrial wastewaters and its removal: A review on biotreatment. *Journal*
474 *of Hazardous Materials*, 2015;163, 1-11
- 475 Tamura, H., Hamaguchi, T., & Tokura, S. "Destruction of rigid crystalline structure to prepare chitin solution",
476 *Advances in chitin science*. 2003;7,84–87.
- 477 Patil, S., Bhole, A., & Natrajan, G. Scavenging of Ni(II) Metal Ions by Adsorption on PAC and Babhul Bark.
478 *Journal of Environmental Science and Engineering*, 2006;48(3), 203-208.
- 479 Volesky, B. (2005). Advances in biosorption of metals: selection of biomass types. *Microbiology Reviews*, 14,
480 291–302.
- 481 Hrapovic, L., & Rowe, R. K. Intrinsic degradation of volatile fatty acids in laboratory- compacted clayey soil.
482 *Journal of Contaminant Hydrology*, 2002;58, 221- 242
- 483 Sasikala, S., & Muthuraman, G. Removal of Heavy Metals from Wastewater Using *Tribulus terrestris* Herbal
484 Plants Powder. *Iranica Journal of Energy and Environment*, 2016;7(1),39-47.
- 485 Baek, K., Song, S., Kang, S., Rhee, Y., Lee, C., Lee, B., Hudson, S., & Hwang, T. Adsorption kinetics of boron
486 by anion exchange resin in packed column bed. *Journal of Industrial Engineering Chemistry*, 2007;13(3), 452-
487 456.
- 488 Kavak, D., & Öztürk, N. Adsorption of boron from aqueous solution by sepirolite: II. Column studies. II.
489 Illusrararasi. *Journal of American Chemical Society*, 2004; 23(25),495-500.
- 490 Aksu, Z., Gönen, F., & Demircan Z. Biosorption of chromium (VI) ions by Mowital®B30H resin immobilized
491 activated sludge in a packed bed: comparison with granular activated carbon. *Process Biochemistry*,
492 2004;38(2),175-186
- 493 Sousa, F. W.. Green coconut shells applied as adsorbent for removal of toxic metal ions using fixed-bed column
494 technology. *Journal of Environmental Management*, 2010;91(8),1634-1640
- 495 Martín-Lara, M. A., Blázquez, G., Ronda, A., Rodríguez, I.L., & Calero, M. Multiple biosorption–desorption cycles
496 in a fixed-bed column for Pb(II) removal by acid-treated olive stone. *Journal of Industrial and Engineering*
497 *Chemistry*, 2012;18(3),1006-1012
- 498
- 499